Disponible en **www.hormigonyacero.com**
Hormigón y Acero 2023; 74(299-300):91-108
https://doi.org/10.33586/hya.2023.3104

Serviceability Limit States According to the New Eurocode 2 Proposal: Description and Justification of the Proposed Changes

Estados Límite de Servicio de acuerdo con la propuesta del nuevo Eurocódigo 2: Descripción y justificación de los cambios introducidos

Alejandro Pérez Caldentey[*,a], Juan Luis Bellod Thomas[b], Lluis Torres[c], Terje Kanstad[d]

[a] *Technical University of Madrid (UPM). FHECOR Consulting Engineers*
[b] *Cesma, Technical University of Madrid (UPM)*
[c] *Universitat de Girona (UdG)*
[d] *Norwegian University of Science and Technology (NTNU)*

Recibido el 8 de septiembre de 2022; aceptado el 26 de enero de 2023

ABSTRACT

In this paper the main changes introduced into FprEN 1992-1-1:2023[1] [1] with respect to the current version of EC2 (EN 1992-1-1:2004) [2] with regard to cracking and deflection calculations are introduced and justified. The changes introduced into the cracking formulation account for the variation of stresses in the tensioned zones for bending, the effect of the casting position and the influence of curvature on the increase of surface crack widths. The introduction of these effects, together with a reformulation of the effective area allow for a reduction of scatter in the model when compared to experimental data. For deflections, a simplified method is introduced which is fully consistent with the general method and allows practical application by providing correction factors to be applied to linear elastic calculations. From this method a formulation for the slenderness limits is deduced. This formulation is the basis for the table-based method to avoid deflection calculations. Finally, coefficients are derived to translate the slenderness limits of beams to the slenderness limits of slabs supported on isolated columns and slabs supported on walls

KEYWORDS: cracking, flexure, tension, deflections, EN 1992-1-1, MC 2010, bond conditions, slabs.

RESUMEN

En este trabajo se introducen y justifican los principales cambios introducidos en la norma FprEN 1992-1-1:2023[2] [1] con respecto a la versión actual del EC2 (EN 1992-1-1:2004) [2] en relación con los cálculos de fisuración y flechas. Los cambios introducidos en la formulación de la abertura de fisura tienen en cuenta la variación de las tensiones en la zona traccionada en flexión, el efecto de la posición de hormigonado y la influencia de la curvatura en el aumento de la abertura de fisura entre el nivel de la armadura y la fibra más traccionada. La introducción de estos efectos, junto con una reformulación del área efectiva, permiten reducir la dispersión del modelo respecto de los datos experimentales. Para las flechas, se introduce un método simplificado que es totalmente coherente con el método general y permite la aplicación práctica al proporcionar factores de corrección que se aplican a los cálculos elástico-lineales. De este método se deduce una formulación para los límites de esbeltez. Esta formulación es la base del método basado en tablas para evitar los cálculos de flechas. Por último, se obtienen coeficientes para extrapolar los límites de esbeltez de las vigas a los límites de esbeltez de losas apoyadas en pilares aislados y de losas apoyadas en muros.

PALABRAS CLAVE: fisuración, flexión, tracción, flechas, EN 1992-1-1, MC 2010, posición de hormigonado, losas.

1.- FprEN 1992-1-1:2023 is available through the National members of CEN TC250/SC2 until approval as EN.
2.- El documento FprEN 1992-1-1:2023 puede obtenerse a través de los miembros nacionales del comité CEN TC250/SC2 hasta que sea aprobado como norma EN.

* Persona de contacto / *Corresponding author*:
Correo-e / *e-mail*: apc@fhecor.es (Alejandro Pérez Caldentey).

How to cite this article: Pérez, A., Bellod, J.L., Torres, L., & Kanstad, T. (2023) Serviceability Limit States According to the New Eurocode 2 Proposal: Description and Justification of the Proposed Changes, *Hormigón y Acero* 74(299/300):91-108, https://doi.org/10.33586/hya.2023.3104

1. INTRODUCTION

The work on the revision of Eurocode 2 started in 2012. The technical content of the revised document was approved by CEN-TC-250/SC2 in June 2022. The revision has therefore taken about 10 years. It is expected that the current draft will be ready for a formal vote in April 2023, but it will still not be fully operational until 2027 since the countries need to draft the National Annexes and there will be a transition period. This standard, when approved, will replace the standard approved in 2004. It can therefore be stated that between revisions of the European standards a period of 25 to 30 years can easily go by.

Some of the goals of the revision were to update the code incorporating the latest state-of the art, improve ease-of-use and reduce the number of nationally determined parameters.

In the revision of Section 7 Serviceability Limit States of EN 1992-1-1:2004 [2] (Section number updated to Section 9), significant changes have been made to the cracking model that allow a reduction in scatter by introducing important effects which have been neglected up to now and can be credited with significant discrepancies between calculated and observed crack width values. These effects have to do with the distribution of stresses (tension or flexure), with the effect of casting position, and with the effects of curvature. These effects will be explained in detail and be illustrated using experimental evidence below. Also, since this is still a matter of controversy in some countries, the importance of accounting for the effect of cover will also be dealt with.

Additionally, content from EN 1992-3:2006 [3] has been incorporated into EN 1992-1-1, particularly considerations regarding the boundary conditions of elements subjected to imposed strains (whether a wall or a slab is restrained at the ends or at the edges.) This should help designers to better understand cracking and how when the restraint is on the edges, the differential strain between steel and concrete is mainly determined by the imposed strain whereas when the element is restrained at the ends, it depends on the cracking load.

Regarding deflections, the general method (ζ-method) has been kept as it was, since it provides relatively good approximations to tests [4] and relies on a robust model. However, in order to improve ease of use, a simplified formulation has been introduced which is consistent with the general method but is much easier to apply by practitioners. This method allows performing a linear elastic calculation to obtain the deflection and correct this calculation to account for cracking and tension stiffening effects. This method also forms the basis for the definition of slenderness limits (span-to-depth ratios).

2. JUSTIFICATION OF THE MODEL FOR THE DETERMINATION OF CRACK WIDTHS

2.1. Main changes in the model

The main changes introduced in the model (see Eq. (1)) are a factor to account for distribution of stresses (k_{fl}) and a factor to account for casting position (k_b), both of which affect the bond term of the crack spacing equation, the introduction into the crack formulation of the curvature factor ($k_{1/r}$) and the formulation of the model in terms of mean values, with an explicit coefficient (k_w) to go from mean crack width values to characteristic values. The reason for this last change is that calibrations can only be meaningfully performed considering the mean values measured in the tests.

Note that the predicted crack width is the crack at the surface of concrete. In the authors' opinion it is important that the formulation describes a magnitude that can be measured so that the formulation may be tested against experimental evidence, which is the basis of the scientific method.

$$s_{r,m,cal} = 1.5c + \frac{1}{7.2}\, k_{fl}\, k_b\, \frac{\phi}{\rho_{s,eff}}$$

$$\varepsilon_{sm} - \varepsilon_{cm} = \frac{\sigma_s - k_t \dfrac{f_{ctm}}{\rho_{eff}}\left(1+\alpha\,\rho_{eff}\right)}{E_c} \geq 0.6\,\frac{\sigma_s}{E_c} \qquad (1)$$

$$w_{k,cal} = k_w\, k_{1/r}\, s_m \left(\varepsilon_{rm,cal} - \varepsilon_{cm}\right) \rightarrow 1.7\, k_{1/r}\, s_{rm,cal} \left(\varepsilon_{sm} - \varepsilon_{cm}\right)$$

In the following the need for these change will be discussed in detail.

2.2. The importance of accounting for cover

There is overwhelming evidence that cover is a significant factor to explain the crack spacing ([5] [6] [7] [8]) and should be explicitly accounted for. This is done by adding a cover term to the bond term when determining the crack spacing. Deniers of this fact have argued that this effect is already accounted for in the definition of the effective area, which, in fact, depends on the cover. However, the tests carried out at the Universidad Politécnica de Madrid in 2009[1] ([7]), clearly demonstrated that this was not enough by testing three pairs of otherwise identical elements (specimens 25-20-XX and 25-70-XX where XX stands for the stirrup spacing in cm going from 00 (no stirrups) to 10 cm and 30 cm) having very different covers (32 and 82 mm) but the nearly same effective area as per the definition included in EN 1992-1-1:2004. The specimens with the higher cover had a maximum crack width opening which was twice as large as that of the specimens with the smaller cover. It was quite notable that for a service stress in reinforcement of only 250 MPa (determined on the basis of a cracked section) the maximum measured crack width was around 0.6 mm, much higher than the values normally deemed admissible (see Figure 1).

There has been an attempt ([9]) to explain this difference by claiming that in Specimens 25-70 the stabilised cracking was not reached whether as in specimen 25-20 it was and therefore different values of the bond strength could explain this behaviour. Unfortunately, this hypothesis is not supported by the experimental data which shows that for both tests

1 All specimens were RC sections subjected to a constant bending zone, having a width of 350 mm, a height of 450 mm, all reinforces with 4 bars in tension. The naming of the specimens is AA-BB-CC, where AA is the bar diameter in tension in mm, BB is the cover to the stirrups in mm (12 mm stirrups) and CC is the stirrup spacing in cm in the constant moment zone area. CC=00 means there are no stirrups.

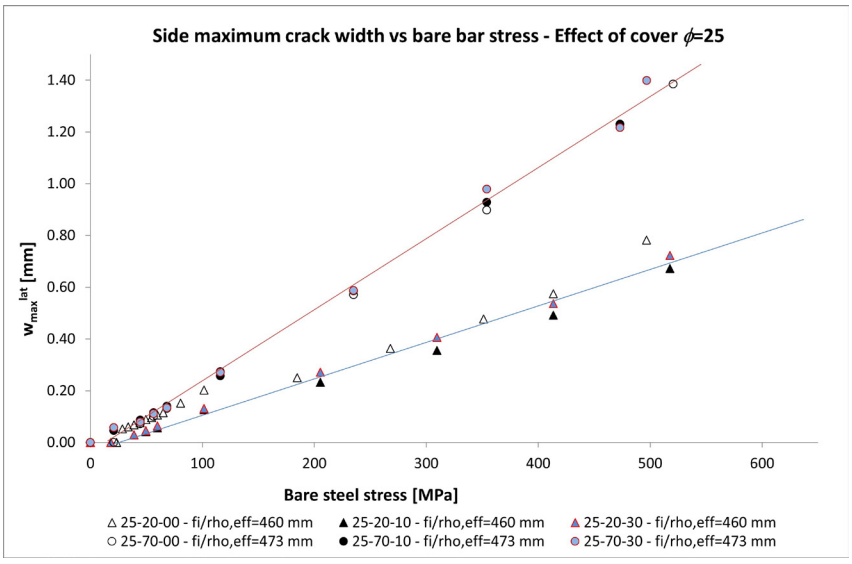

Figure 1. Maximum crack width measured in identical specimens with different covers and nearly the same effective area [7]. The maximum crack within the specimens with larger cover doubles the maximum crack width in the specimens with the smaller cover. The crack width, w_{max}^{lat} is measured at the side of the beam at the level of the tension reinforcement.

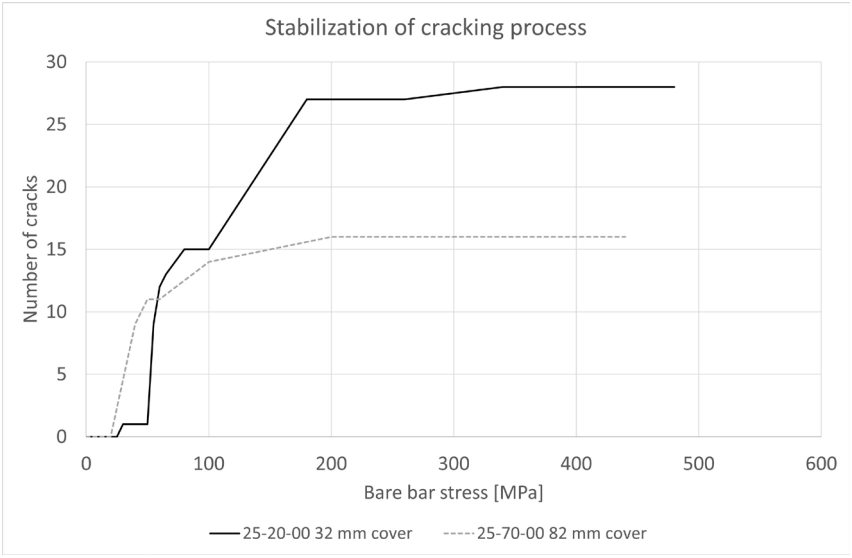

Figure 2. Number of cracks as a function of the steel stress for specimens 25-20-00 and 25-70-00. The crack pattern is stabilized for a stress in steel of about 200 MPa.

stabilized cracking is reached at a stress in the reinforcement of about 200 MPa, as shown in Figure 2.

Given this information, the authors of this paper consider the need for an additive cover term to be a settled matter. The physical explanation for this term is that internal cracks (Goto cracks) form at each rib. A larger proportion of these cracks tend to close before reaching the surface for elements with larger covers. This effect is not modelled by bond theory and thereby requires the corresponding correction in the form of an additive cover term.

2.3. *Effect of casting position*

It is a well-established fact (e.g., see [2], [10], and [11]) that casting position affects the required anchorage length of reinforcing bars. In ULS, the anchorage length has traditionally been increased by a factor of 1.4 for bars in horizontal elements which are close to the top surface. This modification has to do with the appearance of voids under the top bars due to plastic settlement and bleeding, which reduces the bond perimeter of the bar. Even though cracking has to do with bond (and a bond factor has been present in codes – for instance factor k_1 in EN 1992-1-1:2004 which accounts for the different bond properties of ribbed and smooth bars) casting position has – to the knowledge of the authors – never been considered in models dealing with crack spacing [12].

However, tests carried out at the Universidad Politécnica de Madrid (UPM), show strong evidence that casting position has a substantial effect on crack spacing. The flexural specimens 12-70-00 and 12-70-F tested in 2009 [7] and 2017 [13], respectively, with identical geometry (though slightly different concrete mix proportions), showed substantial differences in crack spacing

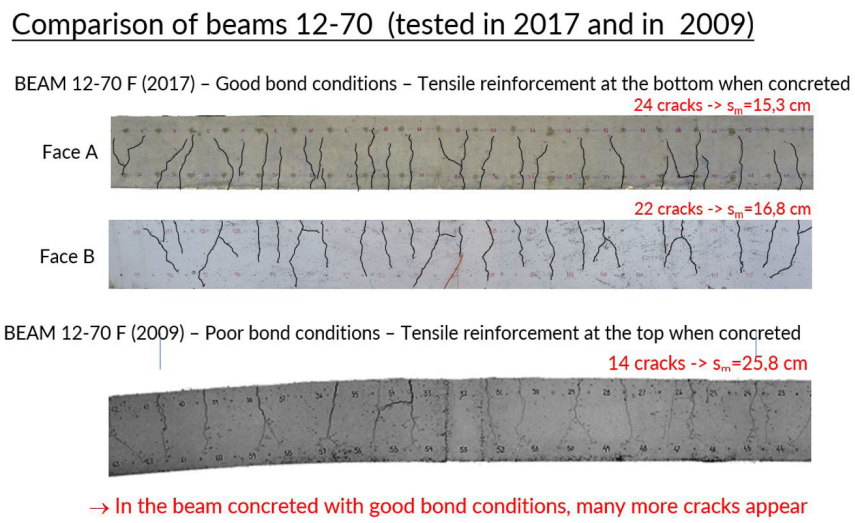

Figure 3. Cracking patterns of beams cast in 'good' casting position (top) and 'poor' casting position (bottom).

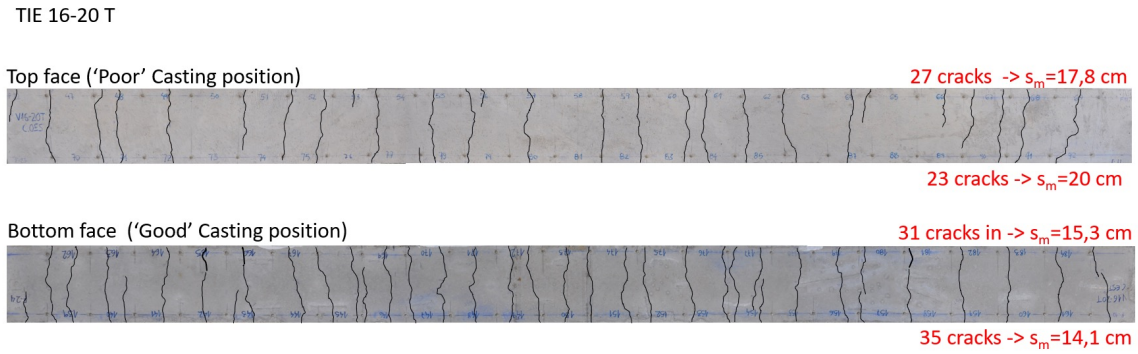

Figure 4. Cracking pattern of a tie showing different crack spacing on different faces.

(see Figure 3). Besides the concrete mix (which is known not to have an important effect on cracking), the only difference was the casting position of the tension reinforcement. In the beam tested in 2009, the tensile reinforcement was cast in 'poor' casting position (top), while in the test carried out in 2017, it was cast in 'good' casting position (bottom). The beam tested in 2009 showed a mean crack spacing of 258 mm, while the element tested in 2017 showed a mean crack spacing of only 161 mm.

The effect of casting position has been confirmed by analysis of the cracking pattern of ties, where the face cast in good casting position has a definite tendency to develop a cracking pattern with more closely spaced cracks. Figure 4[2] also illustrates this fact using results of specimen 16-20-T tested in 2017.

Given this evidence a more systematic study was undertaken at the Universidad Politécnica de Madrid [14]. In this study companion flexural tests were performed in good casting conditions for flexural specimens previously tested in poor casting conditions. Additionally for one of the tests, 25-20-B, the earlier with poor bond conditions was repeated. The results of this study, which includes tests carried out in 2009, 2017, 2018 and 2020, are summarized in Table 1. In all cases, the face concreted in poor conditions showed a larger crack spacing when compared to the face of the corresponding specimen concreted in good bond conditions. Additionally, the table shows that workmanship has a significant influence on this effect. For specimen 25-20-B, the increase in elements concreted in the laboratory is only 11.3%, while the effect is 51.1% when comparing with an element cast on site with poor bond conditions.

While the effect of bond conditions on cracking is clear from these results, it has not been studied before. Because of this the evidence is still scant and does not allow the formulation of an experimentally validated model, even though the results clearly show an effect of the workmanship, as noted above, and possibly an effect of the bar diameter and the cover. Because of the lack of data, the new formulation proposes fixed-value coefficients which are meant to be a recognition that this effect exists and that need to be improved in the future as further data becomes available. The effect is therefore accounted for by a coefficient k_b, which affects the bond term of the crack spacing equation and adopts a value of 0.9 for good bond conditions and 1.2 for poor bond conditions.

2.4. Effect of the distribution of stresses

A new coefficient is suggested to model the effect of uneven distribution of stresses when dealing with elements subjected to bending.

2 The beam was rotated when tested so that the two faces shown were subjected to identical forces from self-weight.

TABLE 1.
Effect of casting position as measured in tests carried out at UPM (taken from [4]).

SPECIMEN	Mean Crack Spacing according to Bond Condition (mm)				
	Good	Poor Lab.	Increase	Poor On-site	Increase
12-20-B-X	115	-	-	173	50.4%
16-20-T-X	147	170.5	16.0%	-	-
16-20-B-X	105	109.8	4.6%	-	-
25-20-T-X	115	171	48.7%	-	-
25-20-B-X	86.7	96.5	11.3%	131	51.1%
12-70-B-X	162	-	-	236	45.7%
16-70-T-X	220	232	5.5%	-	-
16-70-B-X	183	188	2.7%	-	-
25-70-T-X	184	230	25.0%	-	-
25-70-B-X	148.3	-	-	227	53.1%
Average	-	-	**16.2%**	-	**50.1%**

To account for this effect, in EN 1992-1-1:2004 [2], the model for crack spacing includes coefficient k_2 defined as follows (Eq. (2)):

$$k_2 = \frac{(\varepsilon_1 + \varepsilon_2)}{2\varepsilon_1} \tag{2}$$

where ε_1 and ε_2 are the greater and lesser tensile strains in the section (ε_2=0 if part of the section is compressed.) With this definition k_2=1.0 in tension and 0.5 in flexure.

The rationale behind the above factor is that, in bending, the transfer length will be shorter because the tension force per meter of width (coloured area in Figure 5) that has to be transferred by bond to the effective concrete area from an existing crack to produce a new crack will be half that in pure tension because the strain of the least tensioned fibre is zero, and therefore the transfer length would also be half. The current Eurocode 2 (EN 1992-1-1:2004) formulation, however, instead of providing small crack spacings in flexure, is calibrated in such a way that the model results in notoriously exaggerated crack spacings for tension elements (see [15] Figure 1).

The above reasoning, as shown in Figure 5, is not sound because what matters is not the stress gradient within the full tensile zone itself but rather the tensile gradient within the effective area around the bar. In a bending element of significant height, the effective area can represent only a small part of the cross-section in tension and the approximation of a tie, as done in MC 2010 [16] can be reasonable. However, in small elements, the model of EC2 would be better. Figure 6 demonstrates that, for tension, the mean stress, σ_{mean}, in the effective area will be f_{ctm} when the next crack occurs. However, in the case of flexure with the simplifying assumption of a linear distribution, the mean stress can be determined as shown in Eq. (3):

$$\sigma_{mean} = \frac{1}{2}\left(f_{ct,eff} + \sigma_{c,min,ef}\right) = \frac{1}{2}\left(f_{ct,eff} + \frac{f_{ct,eff}}{h - x_g}\left(h - x_g - h_{c,eff}\right)\right) =$$

$$= f_{ct,eff} \underbrace{\frac{1}{2}\left(1 + \frac{(h - x_g - h_{c,eff})}{h - x_g}\right)}_{k_{fl}} \tag{3}$$

where x_g is the depth of the neutral axis in the uncracked section and k_{fl} is the coefficient accounting for the distribution of stresses. This expression results in a value for k_{fl} of 1.0 for pure tension (x_g=∞) and of 0.5 in pure flexure if $h_{c,ef}$ is equal to (h-x_g).

For a rectangular cross section and pure bending, the expression for k_{fl} of Eq. (3) simplifies to Eq. (4):

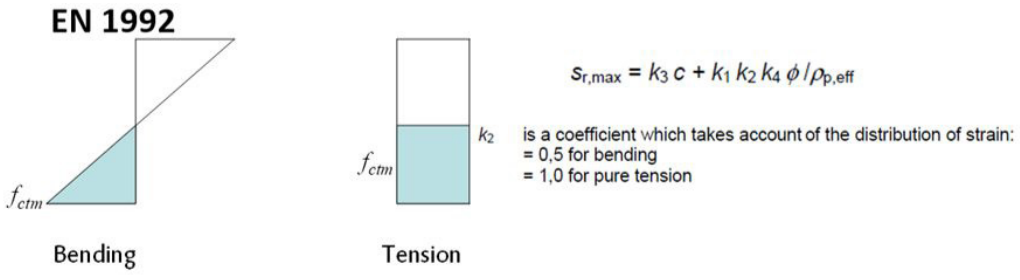

Figure 5. Effect of distribution of stresses prior to cracking on transfer length according to EN 1992-1-1:2004.

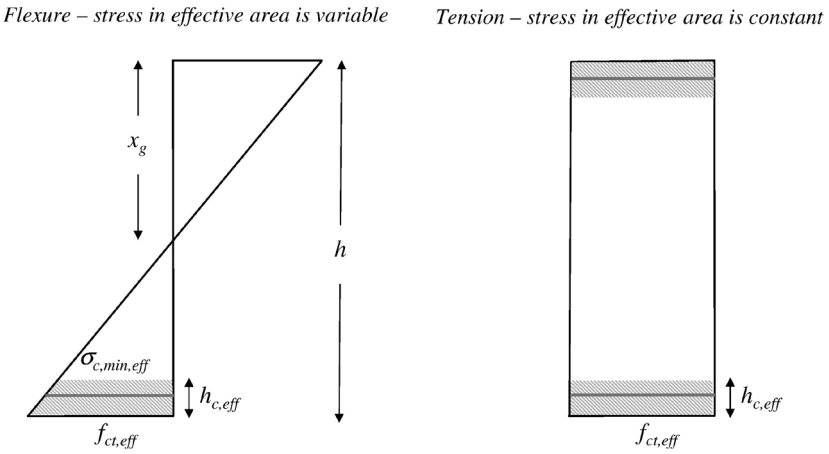

Figure 6. Consideration of the effective tensile area around a bar in flexural elements.

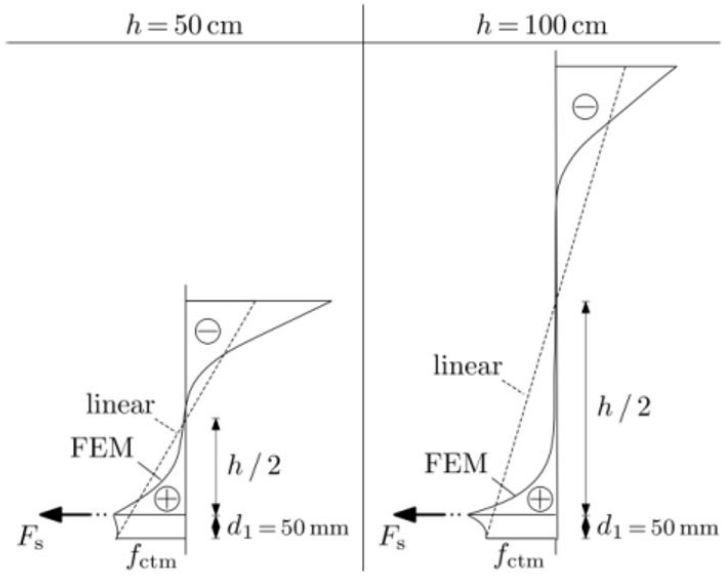

Figure 7. FEM estimate of stresses between cracks [9]. For smaller heights, the stress distribution tends to be triangular whereas for larger elements the is a stronger stress concentration. This behaviour is consistent with the simplified proposal for k_{fl}.

$$k_{fl} = \frac{1}{2}\left(1+\frac{(h-x_g-h_{c,eff})}{h-x_g}\right) = \frac{1}{2}\left(1+\frac{\left(\frac{h}{2}-h_{c,eff}\right)}{\frac{h}{2}}\right) = \frac{1}{2}\left(2-\frac{2h_{c,eff}}{h}\right) = \frac{h-h_{c,eff}}{h} \quad (4)$$

This approach is, of course simplified, since it assumes that the distribution of stresses within the effective area is linear and follows Navier's law. This, of course, is not strictly true. Nonetheless, recent FEM calculations [9] show that the assumption of a constant stress within the effective area is not correct and that the actual distribution of stresses becomes more similar to a triangular distribution as the height of the section is reduced, while it becomes more concentrated as the height increases (see Figure 7). The proposed simplified model is consistent with these findings.

The need to distinguish between elements subjected to flexure and tension has been shown very clearly in [14] from which Table 2 is adapted. The table shows results from several tests, all involving a b x h = 350 x 450 mm rectangular section coded with the bar diameter in tension (4 bars), followed by the cover to the stirrups (for the cover to the longitudinal bars, add 12 mm), type of test (B=bending, T=tension) and the casting position (G=good, PL=Poor in Laboratory conditions).

In Model Code 2010 [16], this effect is accounted for, in an obscure way, by limiting the height of the effective area around a bar in bending to (h-x)/3, whereas there is no such limit in tension. As far as the authors are aware there is no published justification for this factor which seems to be originating from curve fitting to test data. Besides the lack of clarity regarding where this factor comes from, it provides very strange differences for the effective area depending on the type of force applied. Figure 8 shows the effective area for one

TABLE 2.
Experimental results comparing stabilized crack spacing in bending and tension tests and predictions by the new version of EN 1992-1-1, the Model Code 2010 and the current version of EN 1992-1-1 (adapted from [14]).

BEAMS	Measured mean crack spacing (mm)			FprEN 1992-1-1:2022			MC 2010			EN 1992-1-1:2004		
	Predicted mean crack spacing (mm)											
	B	T	Inc. (T-B)/B	B	T	Inc. (T-B)/B	B	T	Inc. (T-B)/B	B	T	Inc. (T-B)/B
12-20-B/T-G	115	162	0.41	137	162	0.18	182	182	0.00	152	240	0.58
16-20-B/T-G	105	147	0.40	125	152	0.22	151	151	0.00	134	203	0.52
16-70-B/T-G	183	220	0.20	213	262	0.23	233	352	0.51	248	477	0.93
16-20-B/T-PL	109.8	170.5	0.55	150	187	0.25	151	151	0.00	134	203	0.52
16-70-B/T-PL	188	232	0.23	243	309	0.27	233	352	0.51	248	477	0.93
25-20-B/T-G	86.7	115	0.33	105	135	0.29	113	119	0.05	110	163	0.48
25-70-B/T-G	148.3	184	0.24	186	245	0.32	175	260	0.49	212	365	0.72
25-20-B/T-PL	96.5	171	0.77	124	164	0.32	113	119	0.05	110	163	0.48
Average	**129**	**175**	**0.39**	**160**	**202**	**0.26**	**169**	**211**	**0.20**	**168**	**287**	**0.64**

of the tests reinforced with 4 25 mm bars and having a cover of 82 mm. The ratio between effective heights is larger than 2.00. This is because the $(h\text{-}x)/3$ limits the height of the effective area for the element subjected to bending. The difference is hard to justify from physical considerations or from what the effective area stands for (i.e. the area of concrete that is effectively tensioned by a bar (or group of bars), or the equivalent area of concrete that has to reach the tensile resistance of concrete for form a new crack adjacent to an existing one, assuming that Navier's hypothesis is valid).

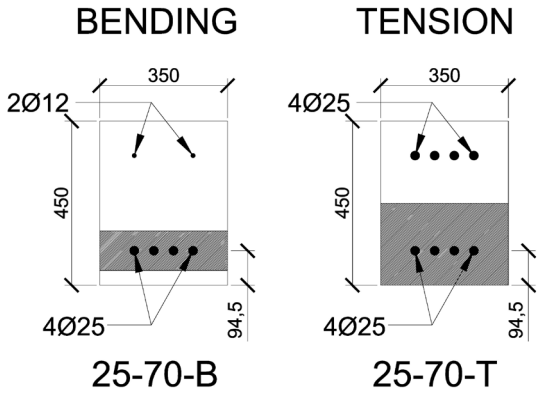

Figure 8. Effective area for specimens with 25 mm diameter and 82 mm cover in bending and tension [7].

Table 2 shows that this factor has no influence for small covers, whereas experimental results report a spacing that is 40% higher in tension than in bending. On the other hand, for large covers, the effect seems to be too large (50% compared to 20 to 33% in experimental results).

In the same table the same results provided by EN 1992-1-1:2004 are given. This model is accounting for the effect of the distribution of stresses twice, once through the limit to the effective area height $(h\text{-}x)/3$ and again through factor k_2. This results in a significant overestimation of the effect of distribution of stresses with the (T-B)/B coefficients ranging from 58% to 72%, much higher than the experimental values.

It is clear that current formulations do not properly account for this effect. Looking at the performance of the proposed method, at first glance, it would seem that while it performs better than the model of EN 1992-1-1:2004 and MC 2010, it still provides rather poor performance. However, it must be considered that this comparison is measuring not only the error in k_{fl}, but also in k_b, the effective area and the calibration coefficients of the cover and bond terms. The comparison can be improved by considering the experimental values of k_b for comparisons referring to the face concreted in poor bond conditions. These values can be obtained from Table 3, below.

The experimental value of k_{fl} can then be obtained for the coarse value of k_b, assuming that this value is the same for the tension and flexural tests as follows ($k_{\phi/\rho}$ is a calibration factor for the slip term):

$$\left.\begin{aligned} s_{r,m,cal,B} - k_c\, c &= k_{\phi/\rho}\, k_{fl}\, k_b\, \frac{\phi}{\rho_{s,eff}} \\ s_{r,m,cal,T} - k_c\, c &= k_{\phi/\rho}\, 1.00\, k_b\, \frac{\phi}{\rho_{s,eff}} \end{aligned}\right\} \rightarrow k_{fl} = \frac{s_{r,m,cal,B} - k_c\, c}{s_{r,m,cal,T} - k_c\, c} \qquad (5)$$

where:

$s_{r,m,cal,B}$ is the calculated mean crack spacing in bending

$s_{r,m,cal,T}$ is the calculated mean crack spacing in tension

The fact is, however, that the experimental k_b factor for the specific tie of the specific flexural element is not the same, so, in order to eliminate this noise from tests performed in poor bond conditions, the k_{fl} can, instead, be obtained accounting for this difference:

$$\left.\begin{aligned} s_{r,m,cal,T} - k_c\, c &= k_{\phi/\rho}\, 1.00\, k_{b,exp,B}\, \frac{\phi}{\rho_{s,eff}} \\ s_{r,m,cal,T} - k_c\, c &= k_{\phi/\rho}\, 1.00\, k_{b,exp,T}\, \frac{\phi}{\rho_{s,eff}} \end{aligned}\right\} \rightarrow k_{fl} = \frac{(s_{r,m,cal,B} - k_c\, c)\; k_{b,exp,T}}{(s_{r,m,cal,T} - k_c\, c)\; k_{b,exp,B}} \qquad (6)$$

Table 3 shows how the "experimental" value of k_{fl} compares with the theoretical value when the noise due to errors in k_b is compensated for in the tests having bars in poor bond position. In the table the ratio of the theoretical value over the experimental value of k_{fl} (th/exp) is given for the case where the value of k_b is taken as either 0.9 or 1.2 ("coarse" value if k_b), as well as for the case when a measured value for k_b is available

TABLE 3.
Evaluation of k_{fl}, accounting for experimental values of k_b tests referring to poor bond conditions.

		coarse value of k_b				*exp value of k_b*			
	kfl, th	**kb**	**kfl, exp**	**th/exp**		**kb, F**	**kb, T**	**kfl,exp,2**	**th/exp**
12-20-B/T-G	0.782	0.9	0.588	1.33		0.90	0.90	0.588	1.33
16-20-B/T-G	0.733	0.9	0.576	1.27		0.90	0.90	0.576	1.27
16-70-B/T-G	0.644	0.9	0.619	1.04		0.90	0.90	0.619	1.04
16-20-B/T-PL	0.733	1.2	0.504	1.45		0.98	1.11	0.571	1.28
16-70-B/T-PL	0.644	1.2	0.596	1.08		0.98	1.01	0.615	1.05
25-20-B/T-G	0.654	0.9	0.578	1.13		0.90	0.90	0.578	1.13
25-70-B/T-G	0.512	0.9	0.415	1.24		0.90	0.90	0.415	1.24
25-20-B/T-PL	0.654	1.2	0.394	1.66		1.13	1.65	0.576	1.14
			Mean =	1.28				Mean =	1.19
			CoV =	16%				CoV =	9%

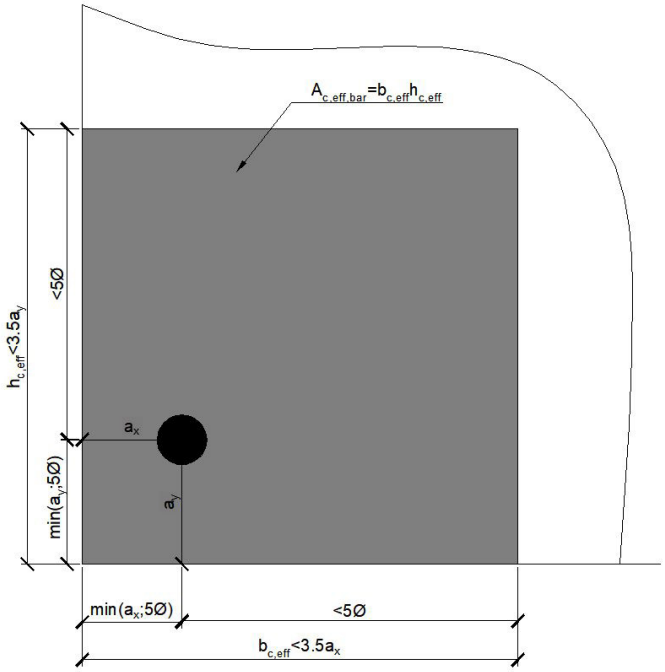

Figure 9. Effective tension area of concrete around an isolated bar, $A_{c,eff,bar}$.

(exp value of k_b). For elements with bars in good bond position this factor does not change, and the base value remains the same. The improvement is significant with the mean value of the ratio between theoretical and experimental results going from 1.28 to 1.19 and the coefficient of variation reducing from 16% to 9%. If anything, these results seem to indicate that the correction for type of loading should be even stronger (lower values of k_{fl}).

2.5. Definition of the effective area of concrete in tension

The definition of the effective tensioned area is changed to account for the removal of the $(h\text{-}x)/3$ limit, to deal with some inconsistencies in its current definition (limit to the area of concrete that is influenced by the presence of the bar) and to contribute to reduce scatter.

For an isolated bar, the proposed definition of the effective area is given in Figure 9 and the following equation:

$$\begin{aligned} &A_{c,eff,bar} = b_{c,eff}\, h_{c,eff} \\ &h_{c,eff} = min\,(a_y + 5\phi; 10\phi; 3.5a_y) \le |h-x| \\ &b_{c,eff} = min\,(a_x + 5\phi; 10\phi; 3.5a_x) \end{aligned} \quad (7)$$

When individual tension areas of different bars overlap, the effective reinforcement ratio should be considered for the group of bars, as shown in Figure 10 and the following equation:

$$\begin{aligned} &A_{c,eff,group} = b_{c,eff}\, h_{c,eff} \\ &h_{c,eff} = min\,(a_y + 5\phi; 10\phi; 3.5a_y) + s_y \le |h-x| \\ &b_{c,eff} = b \end{aligned} \quad (8)$$

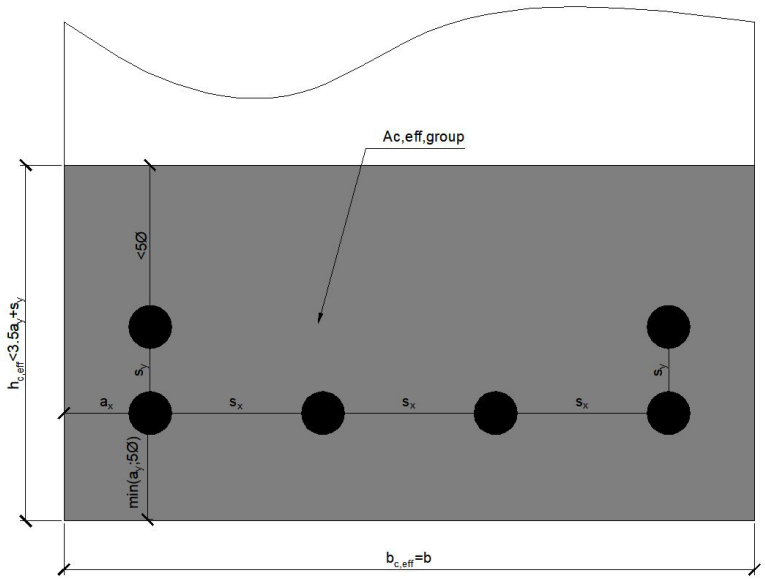

Figure 10. Effective tension area of concrete around a group of bars, $A_{c,eff,group}$ (to be applied when effective tension areas of adjoining bars overlap).

Even though for the example of Figure 10, the strict definition given for the isolated bar would result in a U shape for the effective area, this has been simplified (on the conservative side) by a rectangle, to improve ease of use.

As mentioned above, a limit on the effective area around a bar is given as a linear function of the bar diameter. This condition accounts for the fact that a bar can only control cracks within its proximity. With the definition of the effective area given in MC 2010 and EN 1992-1-1:2004, a single bar placed in the middle of a large rectangle of concrete would have an effective area equal to the area of concrete, and the value of the effective area would increase indefinitely with the dimensions of the cross section. This does not make sense and a limit is therefore necessary for consistency.

2.6. Effect of curvature on crack width

Regarding crack width, it has been well established that, in bending, the value of the crack opening increases from the level of the reinforcement towards the most tensioned face (see for instance the tests reported in reference [7]). The increase in the crack opening is proportional to coefficient $k_{1/r}$, defined, as follows:

$$k_{\frac{1}{r}} = \frac{h-x}{d-x} \tag{9}$$

where:

h is the section height
d is the effective depth, and
x is the depth of the neutral axis of the cracked section

As an illustration, Figure 11 shows a typical example of the accuracy of this correction using one of the tests carried out at UPM (specimen 25-20-00 [7]). The maximum crack width measured at the level of the reinforcement on the side of the beam is plotted against the maximum crack width measured over the exterior bar at the top of the section, both vertical and horizontal covers being the same (32 mm). A nearly per-

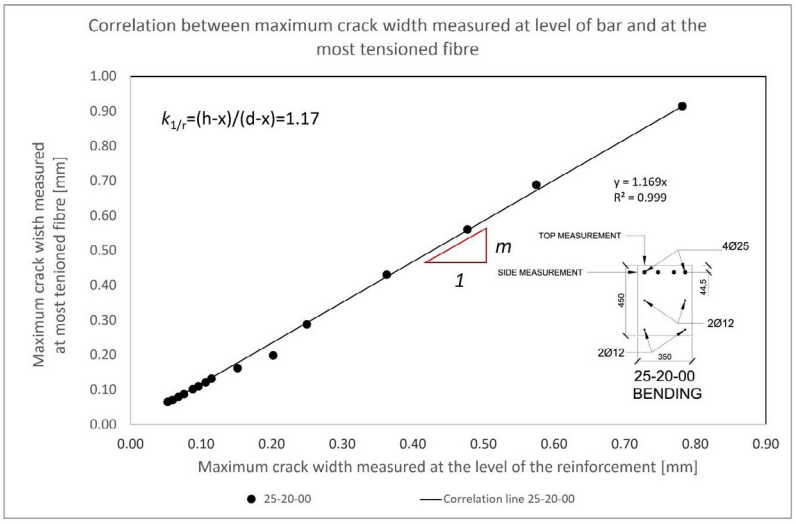

Figure 11. Illustration of the performance of factor $k_{1/r}$ on one of the tests.

TABLE 4.
Comparison between the slope of the correlation line (m) and factor $k_{1/r}$ for all flexural tests performed at UPM (s_t is the stirrup spacing).

Test	c [mm]	Reinf.	st [m]	h [m]	d [m]	x [m]	$k_{1/r}$	m	R^2	$m/k_{1/r}$
12-20-00	32	4•12	-	0.45	0.412	0.077	1.11	1.09	0.998	0.98
12-20-10	32	4•12	0.2	0.45	0.412	0.077	1.11	1.15	0.995	1.03
12-20-30	32	4•12	0.3	0.45	0.412	0.077	1.11	1.10	1.000	0.99
12-70-00	82	4•12	-	0.45	0.362	0.071	1.30	1.29	1.000	0.99
12-70-10	82	4•12	0.2	0.45	0.362	0.071	1.30	1.32	1.000	1.01
12-70-30	82	4•12	0.3	0.45	0.362	0.071	1.30	1.32	1.000	1.01
16-20-00	32	4•16	-	0.45	0.410	0.094	1.13	1.13	0.993	1.00
16-70-00	82	4•16	-	0.45	0.360	0.089	1.33	1.34	0.985	1.00
25-20-00	32	4•25	-	0.45	0.406	0.141	1.17	1.17	1.000	1.00
25-20-10	32	4•25	0.2	0.45	0.406	0.141	1.17	1.24	0.997	1.06
25-20-30	32	4•25	0.3	0.45	0.406	0.141	1.17	1.26	1.000	1.08
25-70-00	82	4•25	-	0.45	0.356	0.132	1.42	1.40	0.995	0.98
25-70-10	82	4•25	0.2	0.45	0.356	0.132	1.42	1.41	1.000	0.99
25-70-30	82	4•25	0.3	0.45	0.356	0.132	1.42	1.32	1.000	0.93
									$\mu =$	1.00
									$\sigma =$	0.036
									CoV =	3.6%

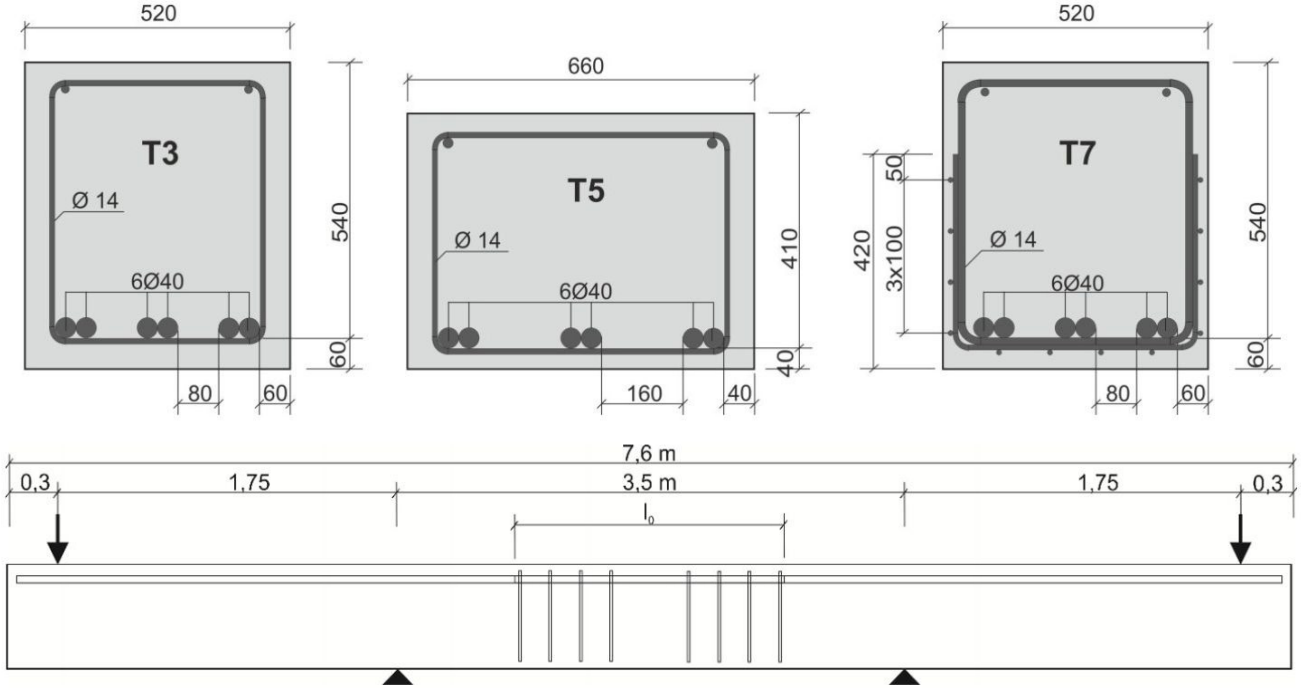

Figure 12. Test set-up and cross section of tests. Figure taken from [18]. Note that the elements were tested with the large reinforcement bars on the top (rotated 180º with respect to the cross sections shown).

fect linear correlation is obtained with a slope which closely mirrors the result obtained by applying the definition of the $k_{1/r}$ factor. This result is not the fruit of chance. Table 4 shows a comparison between the slope of the correlation line, m, determined as in Figure 11 and the value of the $k_{1/r}$ factor for all the flexural tests carried out at UPM until now (14 tests). The ratio between these two values is always very close to 1.00 and the coefficient of variation is only 3.6%. This is a clear indication that this factor is quite accurate and very necessary if an adequate estimate of the surface crack is to be obtained.

This factor is particularly necessary when estimating the crack width of flexural elements with large bars. Typically, such elements have large covers and large reinforcement ratios resulting in large values of x, and thereby in large values of the $k_{1/r}$ factor. This can be illustrated with the tests carried out by Hegger *et al.* [17] (also reported in [18]). These tests involve large bar diameters (from 40 to 60 mm) and covers ranging from 40 to 75 mm. Figure 12 shows the test set-up as well as the definition of the sections. Figure 13 shows the comparison between mean crack openings predicted by the model of FprEN1992-1-1:2022 and those actually measured. A good approximation is obtained with the correlation slope being close to 1.00 and having a high coefficient of determination. The mean value of the ratio of mean calculated to mean

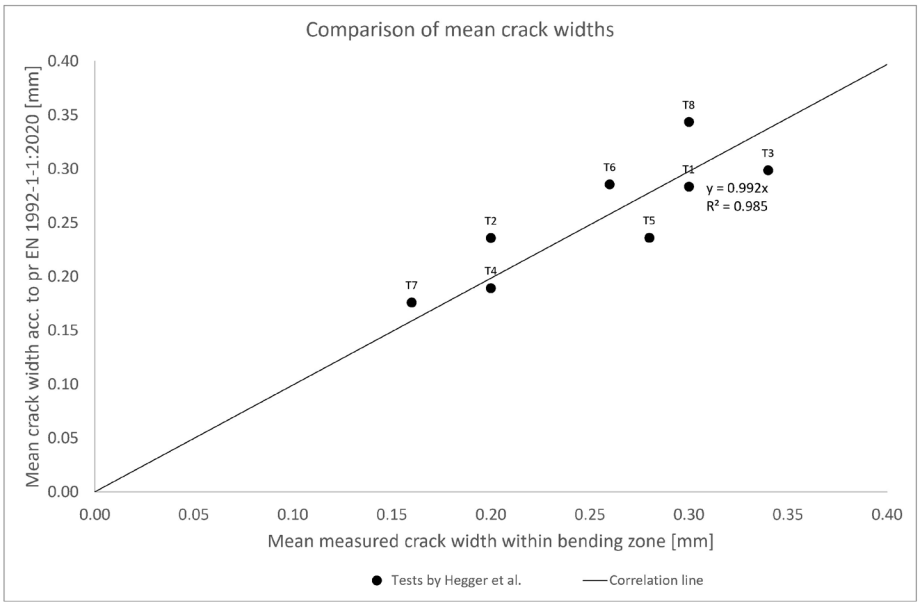

Figure 13. Comparison between mean crack width predicted by the model of FprEN1992-1-1:2022 [1] and the values measured experimentally.

experimental crack width ($w_{m,calc}/w_{m,exp}$) is 1.01 and the CoV is 12.4%. This result is independent experimental confirmation of the performance of the model since these tests were not considered for the calibration of the model.

This model can also easily account successfully for the effect of adding surface reinforcement to control crack width in elements reinforced with large diameter bars and can be used to justify experimental rules (see [19]). The main reasons why the introduction of surface reinforcement reduces the crack widths are the reduction of cover, the reduction in factor $k_{1/r}$, the increase in the effective reinforcement ratio, and, to a lesser extent the reduction in the equivalent bar diameter and the increase in total reinforcement, this last factor having a very minor effect. Also note that k_{fl} increases because $h_{c,eff}$ decreases.

2.7. Type of restraint

It is well known that elements that are subjected to imposed deformation and restrained at ends are subjected, at most, to the cracking force. This is because the magnitude of the imposed strains that are found in normal structural concrete applications are small enough for the element to be in the crack formation stage. As the imposed strain increases, when the stress in concrete between cracks reaches the tensile strength of concrete, a new crack forms and the forces are reduced because the stiffness is reduced. New cracks will form each time this happens as the imposed strain increases. Therefore, the cracking force is the maximum force that can develop in the element with restrained ends. This behaviour is possible because the formation of a new crack affects the distribution of forces in the whole element.

When the element is restrained at the edges, the behaviour is different, because compatibility cannot be achieved globally as in the previous case but has to be met locally because the length of the edge does not change. The formation of a crack does not relieve stresses at a certain distance from the crack so that cracks form independently from one another. Figure 14 shows the behaviour in this case[3]. Ignoring tension stiffening effects, if s_r is the distance between two cracks the concrete between the cracks would shrink a length equal to the imposed deformation and therefore the crack opening would be $s_r \varepsilon_{imp}$. So, the crack opening is no longer a function of the steel stress but a function of the imposed deformation. Accounting for tension stiffening effects, the relative strain between steel and concrete can be expressed as in Eq. (10). If the edges are not totally restrained the imposed deformation is obtained by multiplying the free imposed strain by a restraint factor which is determined from a linear elastic analysis which accounts for the flexibility of the restraint in which the free strain is applied on the structure. The restraint factor is a function of the ratio between the strain that develops freely in the element and the imposed strain.

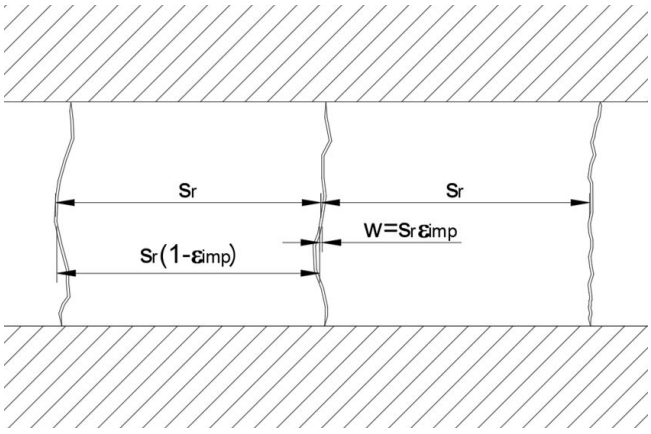

Figure 14. Cracking: behaviour of an element retrained at the edges. It is assumed that the edges are fully restrained. Tension stiffening effects are not included.

3 The behaviour is simplified here for the purpose of explanation. In actual structures the stabilized crack pattern will normally not have been achieved and the adjacent cracks would normally not be formed. s_r would represent the transfer length in such a case.

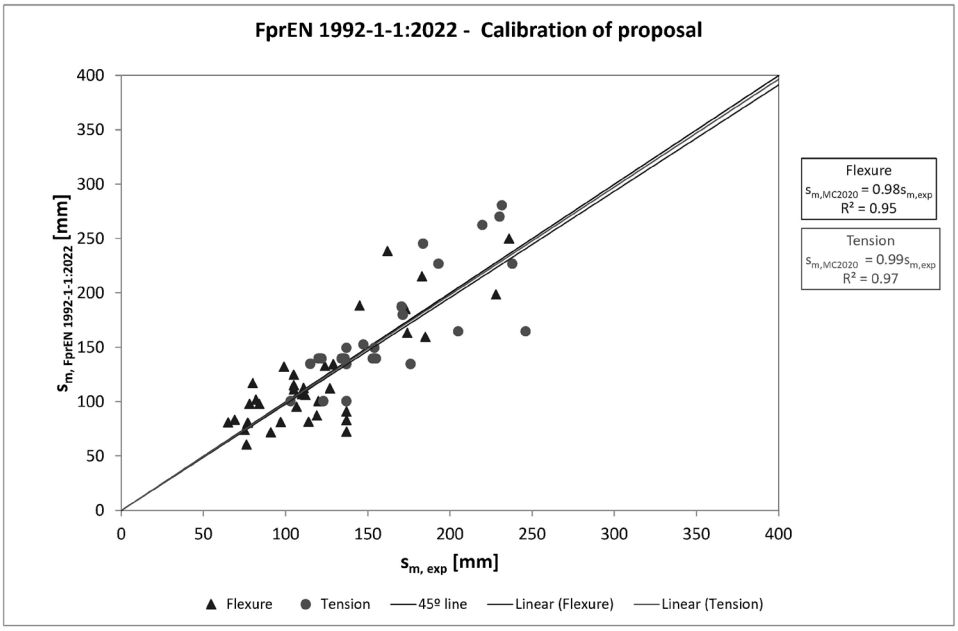

Figure 15. Comparison between predicted and measured crack spacing, separated according to type of load.

$$\varepsilon_{sm} - \varepsilon_{cm} = \varepsilon_{imp} - k_t \frac{f_{ct,eff}}{E_{cm}}$$
$$\varepsilon_{imp} = R_{ax}\, \varepsilon_{free} \qquad (10)$$

where:

R_{ax} is the restraint factor, which is obtained as $R_{ax} = 1 - \frac{\varepsilon_{restr}}{\varepsilon_{imp}}$, where ε_{restr} is the strain that develops freely in the restrained element and ε_{imp} is the imposed strain (e.g. free shrinkage, free temperature strain).

2.8. Calibration and comparison

The formulation has been calibrated to determine the coefficients to be applied to the cover term and the bond term. The expressions for the mean crack spacing can be written as follows:

$$s_{r,m,cal} = k_c c + k_{\phi/\rho} k_{fl} k_b \frac{\phi}{\rho_{s,eff}}\ , \qquad (11)$$

where:

k_c is an empirical parameter account for the influence of the concrete cover not accounted for in the bond term; as a simplification, k_c = 1.5 can be assumed;

c is the maximum concrete cover. The maximum value has been adopted because recent research [20] confirms that, when vertical and horizontal covers are different, crack spacing is much better correlated to the maximum cover than to minimum cover. When the effective area concept applies to a single bar located in the perimeter of the section, the maximum cover of this bar applies. When the effective area applies to a group of bars, the most unfavourable value of cover of the bars located in the perimeter of the section should be considered;

$k_{\phi/\rho}$ is an empirical parameter to account for the influence of bond; as a simplification, $k_{\phi/\rho}$ =1/7.2 can be assumed.

The design crack width is obtained from Eq. (12).

$$w_{k,cal} = k_w\, k_{1/r}\, s_{r,m,cal} \left(\varepsilon_{sm} - \varepsilon_{cm}\right) \qquad (12)$$

where:

k_w is a factor to obtain a design value of the crack width from the mean value, which can be taken as 1.7;

ε_{sm} is the average steel strain over the length $s_{r,m,cal}$;

ε_{cm} is the average concrete strain over the length $s_{r,m,cal}$;

For members subjected to direct loads (stabilized cracking) or for members subjected to imposed strains (crack formation phase) restrained at the ends, $\varepsilon_{sm}-\varepsilon_{cm}$ can be determined as in Eq. (13).

$$\varepsilon_{sm} - \varepsilon_{cm} = \frac{1}{2}\left(\sigma_s - k_t \frac{f_{ct,eff}}{\rho_{ct,eff}}\left(1 + \alpha_e\, \rho_{eff}\right)\right) \qquad (13)$$

where:

E_s is the modulus of elasticity of steel;

σ_s is the stress of steel at the crack;

k_t is an empirical coefficient to assess the mean strain over the transfer length, equal to 0.6 for short-term analysis and equal to 0.4 for long-term analysis or repeated loading;

$f_{ct,eff}$ is the effective tensile strength of concrete, which in practical cases can be taken as the mean tensile strength $f_{ct,m}$;

α_e is the modular ratio=E_s/E_c;

For members subjected to imposed strains and restrained at the ends, the applied load is assumed to be the cracking force and the parenthesis in Eq. (13) simplifies to:

$$\left(\sigma_s - k_t \frac{f_{ct,eff}}{\rho_{eff}}\left(1 + \alpha_e\, \rho_{eff}\right)\right) = \frac{f_{ct,eff}}{\rho_{s,eff}}\left(1 + \alpha_e\, \rho_{eff}\right)\left(1 - k_t\right) \qquad (14)$$

TABLE 5.
Statistical analysis of crack spacing.

		MC 2010		EN 1992-1-1:2004		FprEN 1992-1-1:2022	
		Flexure	Tension	Flexure	Tension	Flexure	Tension
	nº of tests	37	36	37	36	37	36
	$\sqrt{(\Sigma\varepsilon^2/N)}$	**38.28**	**37.96**	**35.25**	**83.01**	**29.01**	**30.97**
Model/Exp.	$min(s_{m,model}/s_{m,exp})$=	0.46	0.51	0.6	0.68	0.53	0.67
	$max(s_{m,model}/s_{m,exp})$=	1.78	1.51	1.74	2.04	1.47	1.34
	μ =	1.04	1.05	1.08	1.43	1.00	1.01
	σ =	0.29	0.22	0.27	0.30	0.24	0.16
	COV =	**27.68%**	**21.18%**	**24.69%**	**21.25%**	**23.57%**	**15.62%**

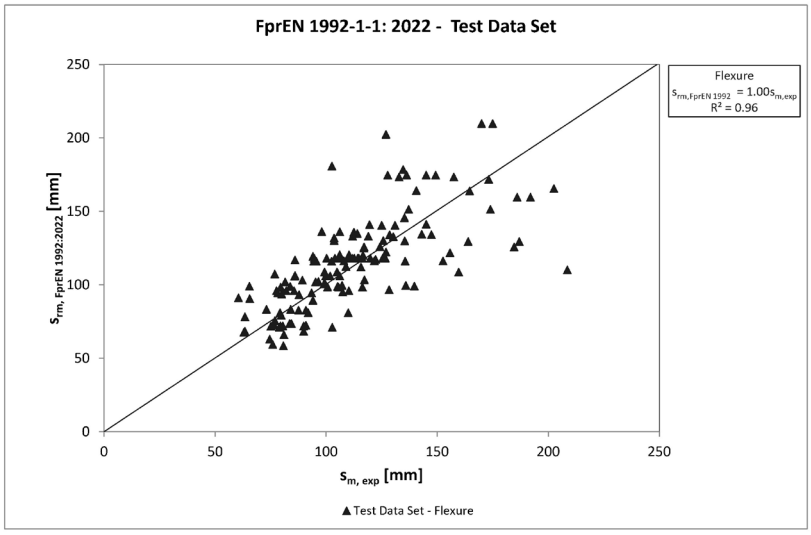

Figure 16. Comparison between predicted and measured crack spacing for the independent test series.

For members subjected to imposed strains and restrained at the edges, $\varepsilon_{sm}-\varepsilon_{cm}$ can be determined as in Eq. (10).

Figure 15 shows the comparison between predicted values, $s_{rm,FprEN1991\text{-}1:2022}$, and experimental values of crack spacing, $s_{m,exp}$. The correlation lines show a coefficient of determination of 0.95 in flexure and 0.97 in tension and a slope close to 1.00. Contrary to the current version of EC2, for which the crack width in tension specimen is overestimated, there is no skew between tension and flexure in the new proposal. This is due to the deletion of the $(h\text{-}x)/3$ limit and the introduction of factor k_{fl}.

Table 5 shows the statistical parameters referred to the 73 tests used for the calibration for crack spacing which includes tests by [21], [22], [23], [24], [7], [13], [25], [26], [27] (see [28]). The table includes the mean squared error, the minimum value of the ratio of model prediction and experimental values (min), its maximum value (max), its mean value (μ), its standard deviation (σ) and its coefficient of variation (COV).

It can be seen the proposed corrections improve the prediction quality in statistical terms, for all the considered statistical parameters, both in flexure and in tension with respect to both the formulation of MC 2010 and EN 1992-1-1:2004. The improvement in tension is related to the changes introduced in the definition of the effective tension area.

2.9. Verification of the calibration using an alternative data set

The model has been calibrated with the same data set (calibration set) as was used for the original calibration of MC 2010, with the addition of several experimental series, as mentioned above. The robustness of this calibration was verified using a separate set of data (test set – see [28]). The independent database includes a total of 144 specimens. This database consists of the following tests:

- Clark (54 specimens) [22]
- Rehm&Rüsch (30 specimens) [25]
- Gribniak (6 specimens) [29]
- Gilbert & Nejadi (12 specimens) [30]
- Calderón (14 specimens) cast in poor casting position [31]
- Wu (4 specimens) – 2 Tests with excessive side cover were discarded [32]
- Frosch (2 specimens) – Other tests with excessive side cover were discarded – Poor casting position [33]
- Case, Beeby (16 specimens) – Tests with mild reinforcement were discarded [34]
- Klakauskas (6 specimens) [35]

The details of the specimens are available in [28].

Figure 16 demonstrates the performance of the proposed model on the independent test set. Even though there is scatter, the model proves to be well-calibrated. Table 6 shows

TABLE 6.
Statistical analysis of crack spacing for the independent data set.

		MC 2010	EN 1992-1-1:2004	FprEN 1992-1-1:2022
	nº of tests	144	144	144
	$\sqrt{(\Sigma\varepsilon^2/N)}$	26.97	26.3	23.55
Model/Exp.	$\boldsymbol{min}(s_{m,model}/s_{m,exp})$=	0.54	0.51	0.53
	$\boldsymbol{max}(s_{m,model}/s_{m,exp})$=	1.87	1.63	1.76
	μ =	1.05	0.99	1.04
	σ =	0.24	0.24	0.2
	COV =	**23.04%**	**24.56%**	**18.85%**

the corresponding statistical parameters. It can be observed that the application of the proposed modification reduces the coefficient of variation from 23.0% for MC 2010 and 24.6% for EN 1992-1-1:2004 to 18.9%. This result corroborates the need for the corrections proposed to account for differences between flexure and tension.

3. DEFLECTIONS

3.1. Simplified method for deflection control

The general method for determining deflection (ζ-method) has been left untouched in the FprEN1992-1-1:2022 [1], because there was no reason to change it as it provides satisfactory results and has a solid basis. However, it is notorious among practicing engineers that this method is not easy to apply to real projects, for which linear models with complex geometries are used. The current practice consists in determining a certain factor to apply to linear elastic calculation in order to obtain an estimate of the deflection considering creep and shrinkage effect. Up to now the determination of this coefficient has been done using approximate methods whose basis is not fully clear. In order to improve ease-of-use, and provide a common basis for this practice, a simplified approach is provided, in which the long term cracked deflection can be easily obtained by taking the linear elastic deflection and correcting with simple coefficients that account for cracking and tension stiffening effects as shown in Eq (15).

$$\delta = k_I\left[\delta_{LOADS} + k_S\,\delta_{\varepsilon_{cs}}\right] \tag{15}$$

The basis of this procedure is an approximation to the long-term ratio between the cracked and uncracked sectional inertia. It results that this ratio can be approximated with significant precision with a fairly simple formulation for rectangular sections. Figure 17 shows this approximation. Note that $\alpha_{e,eff}$ is the long term modular ratio, which accounts for creep (see Eq. (16)).

$$\alpha_{e,eff} = \frac{E_s}{E_c}(1+\varphi) = \frac{E_s}{E_{c,eff}} \tag{16}$$

The creep coefficient can be taken as weighted mean value (φ_{mean}) according to the following expression:

$$\varphi_{mean} = \frac{\varphi(t, t_0)g_{SW} + \varphi(t, t_1)g_{SDL} + \varphi(t, t_2)\psi_2 q_{LL}}{g_{SW} + g_{SDL} + \psi_2 q_{LL}} \tag{17}$$

where:

g_{SW} is the self-weight, applied when the concrete age is t_0;
g_{SDL} is the superimposed dead load applied when the concrete age is t_1;
$\psi_2 q_{LL}$ is the quasi-permanent live load applied when the concrete age is t_2;
t is the age of concrete corresponding to the service life of the structure.

Using the approximation to the ratio I_{cr}/I_g shown in Figure 17, and applying the methodology of the ζ-method which consists in interpolating a stiffness between the fully cracked and uncracked values, factor k_I is determined as shown in Eq. (18).

$$\zeta = \left(1 - 0.5\left(\frac{M_{cr}}{M_k}\right)^2\right)$$

$$K_I = \zeta\frac{I_g}{I_{cr}} + (1-\zeta) = \zeta\frac{1}{2.7\,(\alpha_{e,eff}\,\rho)^{0.6}}\left(\frac{h}{d}\right)^3 + (1-\zeta) \tag{18}$$

The deflection due to shrinkage is obtained by applying a constant shrinkage strain on the structure, determining the elastic deflection, and correcting this by a coefficient that takes into account how the ratio between the equivalent and the uncracked first order moment of the reinforcement with respect to the centroid of the cross section changes due to cracking and tension stiffening effects. The correction in this case is given in Eq. (19). Figure 18 shows calculated values of this ratio for 3 different concrete strengths and the proposed approximation as a function of the reinforcement ratio.

$$k_s = 455\rho^2 - 35\rho + 1.6 \tag{19}$$

3.2. Slenderness limits for beams

Eq. (15) can easily be converted into a general formulation to determine the slenderness limit. Eq. (20) shows the condition for the slenderness limit, i.e., that the deflection be limited to a fraction ($1/a$) of the span (where a is usually taken as 250). It also shows the expressions of the deflections due to a uniformly distributed load and to a constant curvature due to shrinkage.

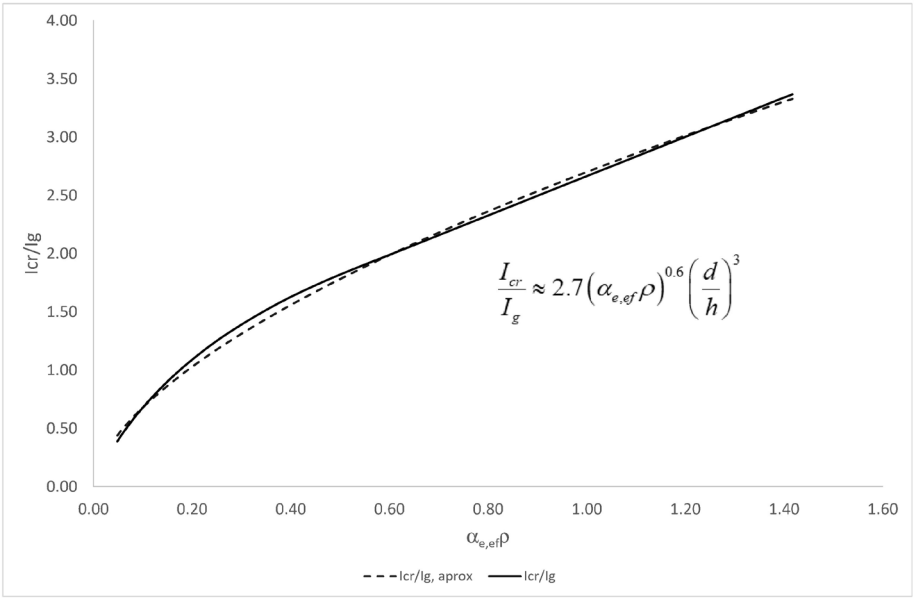

Figure 17. Ratio between long term cracked inertia and gross cross sectional inertia as a function of the long-term transformed reinforcement ratio.

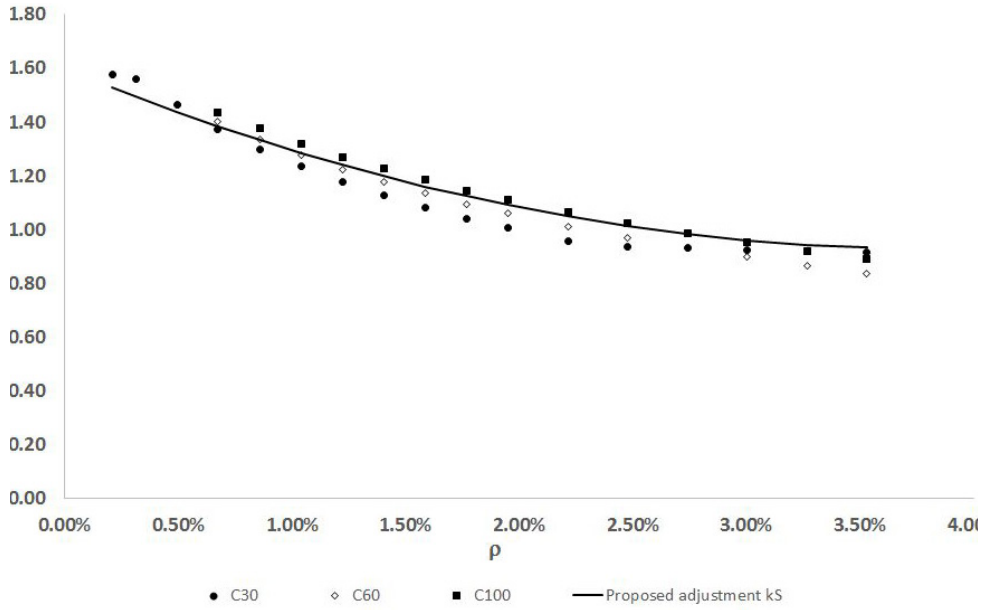

Figure 18. Ratio between the equivalent and the uncracked first order moment of the reinforcement with respect to the centroid of the section as a function of the reinforcement ratio for different concrete strengths.

$$\delta = k_I\left[\delta_{LOADS} + k_S\delta_{\varepsilon_{cs}}\right] \le \frac{L}{a}$$

$$\delta_{LOADS} = K\frac{5}{384}\frac{q_{qp}L^4}{E_{c,eff}\frac{1}{12}bh^3} \qquad (20)$$

$$\delta_{\varepsilon_{cs}} = K_{cs}\varepsilon_{cs}\frac{E_s}{E_{c,eff}}\frac{A_s\left(d-\frac{h}{2}\right)-A_s\left(\frac{h}{2}-(h-d)\right)}{\frac{1}{12}bh^3}\frac{L^2}{8}$$

where:

K is a factor that considers the support conditions for the deflection due to uniformly distributed loads and can be determined from Eq. (21) (for a detailed derivation see [36]):

$$K = \sqrt[3]{\frac{f_{simply,sup}}{f_{real,sup,cond}}} \qquad (21)$$

where:

$f_{simply,sup}$ is the linear elastic deflection of the simply supported member of arbitrary span subjected to a uniformly distributed load, and

$f_{real,sup,cond}$ is the linear elastic deflection of the member with the actual support conditions with the same arbitrary span and subjected to the same uniformly distributed load.

K_{cs} is a factor that considers the support conditions for the deflection due to shrinkage and can be determined from Expression (22) (for a detailed derivation see [36]):

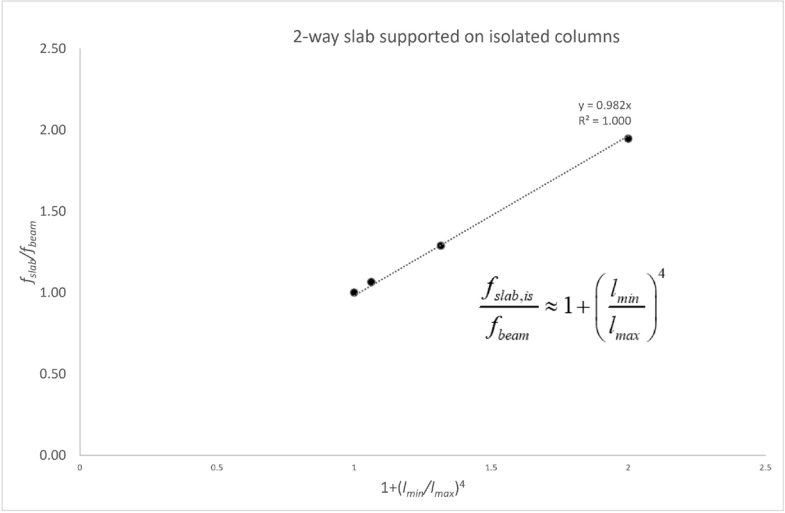

Figure 19. Ratio of the elastic deflection of a slab supported on 4 isolated columns and a simply supported beam as a function of parameter $1+(l_{min}/l_{max})^4$.

$$K_{cs} = \frac{f_{simply,sup}}{f_{cs,real,sup,cond}} \tag{22}$$

where:

$f_{cs,simply,sup}$ is the linear elastic deflection of the simply supported member of arbitrary span subjected to a constant curvature, and

$f_{cs,real,sup,cond}$ is the linear elastic deflection of the member with the actual support conditions with the same arbitrary span and subjected to a constant curvature.

Assuming that the provided reinforcement is that strictly needed in ULS, the value of the quasi-permanent load of a simply supported element can be determined from the ultimate bending resistance as shown in Expression (23) as the product of the ultimate load and coefficient k_{DL} ($q_{qp}=k_{DL}q_{Rd}$).

$$M_{Rd} = q_{Rd}\frac{L^2}{8} = A_s f_{yd}\left(d-0.5\frac{A_s f_{yd}}{bf_{cd}}\right)$$

$$q_{Rd} = A_s f_{yd} d\left(1-0.5\underbrace{\frac{A_s f_{yd}}{bf_{cd}}}_{\omega}\right)\frac{8}{L^2} \tag{23}$$

$$\frac{q_{qp}}{q_{Rd}} = \frac{G+\psi_2 Q}{\gamma_G G+\gamma_Q Q} = \frac{\frac{\left(1-\frac{LL}{TL}\right)}{\frac{LL}{TL}}+\psi_2}{\gamma_G\frac{\left(1-\frac{LL}{TL}\right)}{\frac{LL}{TL}}\gamma_Q} = \frac{\left(1-\frac{LL}{TL}\right)+\psi_2\frac{LL}{TL}}{\gamma_G\left(1-\frac{LL}{TL}\right)+\gamma_Q\frac{LL}{TL}} = k_{DL}$$

$$\frac{LL}{TL} = \frac{Q}{G+Q} \rightarrow G = \frac{\left(1-\frac{LL}{TL}\right)}{\frac{LL}{TL}}Q$$

In Expression (23) it is assumed that there is no need for compression reinforcement in ULS.

Introducing the value of q_{qp} into Expression (20), and developing, the slenderness limit can be obtained as shown in Expression (24). This expression also assumes that there is no compression reinforcement but can be easily generalized for this case (see [36]). However, the effect of compression reinforcement on deflections is limited, and the increase in precision for this rare case is not worth the complication.

$$k_I\left[\begin{array}{l} K\frac{5}{384}\frac{k_{DL}A_s f_{yd} d\frac{8}{L^2}(1-0.5\omega)L^4}{E_{c,eff}\frac{1}{12}bh^3} \\ \\ +k_s K_{cs}\varepsilon_{cs}\frac{E_s}{E_{c,eff}}\frac{A_s\left(d-\frac{h}{2}\right)-A'_s\left(\frac{h}{2}-(h-d)\right)}{\frac{1}{12}bh^3}\frac{L^2}{8} \end{array}\right] \le \frac{L}{a} \tag{24}$$

$$\left.\begin{array}{l} q_{qp} = k_{DL}q_{Rd} = k_{DL}A_s f_{yd} d(1-0.5\omega)\frac{L^2}{8} \\ A'_s = 0 \end{array}\right\} \rightarrow$$

$$\frac{L}{d} \le \frac{E_{c,eff}}{k_1 12a}\left(\frac{h}{d}\right)^3\left[\frac{1}{Kk_{DL}\frac{5}{48}f_{cd}\omega(1-0.5\omega)+k_s K_{cs}\varepsilon_{cs}\frac{E_s}{8}\rho\left(1-\frac{h}{2d}\right)}\right]$$

The values included in Table 9.3 of FprEN 1992-1-1:2022 are derived from this expression assuming that the concrete class is C30, that a is 250 and that the quasipermanent live load is 30% of the total live load. The creep coefficients implicit in k_I were determined assuming the following conditions:

- The self-weight is applied at 7 days
- The superimposed dead load is 15% of the self-weight and is applied at 60 days
- The quasi-permanent live load is applied at 365 days
- The relative humidity is 50%
- The deflection is determined for a design life of 100 years

3.3. *Slenderness limits for slabs*

The Slenderness limits for slabs on isolated supports and on continuous supports can be obtained by multiplying the values

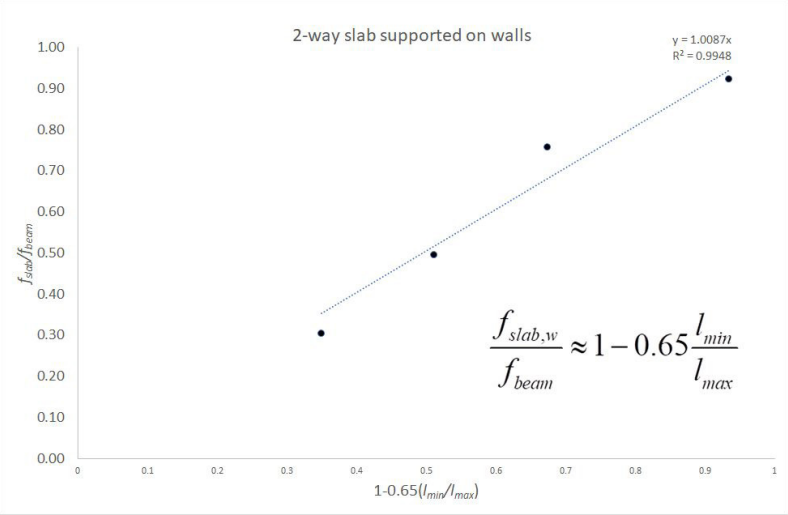

Figure 20. Ratio of the elastic deflection of a slab supported on walls and a simply supported beam as a function of parameter $1+0.65l_{min}/l_{max}$

of Table 9.3 by coefficients which are determined from the ratio of the linear elastic deflections of the slab and a simply supported beam of the same span.

Figure 19 shows that the ratio is a linear of the fourth power of the ratio between the shorter and longer spans. The ratio corresponding to the slenderness limits of the two support conditions (factor K) can the easily be determined as shown in Eq. (25):

$$f_{slab,is} \approx \left(1+\left(\frac{l_{min}}{l_{max}}\right)^4\right) f_{beam,\,l_{max}} = f_{beam,\,l_{beam}} \tag{25}$$

$$\rightarrow \left(1+\left(\frac{l_{min}}{l_{max}}\right)^4\right) k\,\frac{q l^4{}_{max}}{EI} = k\,\frac{q l^4{}_{beam}}{EI} \rightarrow \frac{l_{min}}{l_{beam}} = \sqrt[4]{\frac{1}{1+\left(\frac{l_{min}}{l_{max}}\right)^4}}$$

$$\rightarrow \frac{\frac{l_{max}}{d}}{\frac{l_{beam}}{d}} = \sqrt[4]{\frac{1}{1+\left(\frac{l_{min}}{l_{max}}\right)^4}}$$

$$\rightarrow \frac{l_{max}}{d} = \frac{l_{beam}}{d}\sqrt[4]{\frac{1}{1+\left(\frac{l_{min}}{l_{max}}\right)^4}}$$

For a slab supported on walls, Figure 20 shows the ratio of the deflection of the slab to the deflection of the simply supported beam as a function of 1-0.65 (l_{min}/l_{max}). The correlation line has a slope very close to 1.00 and a high coefficient of determination. With identical reasoning as above, the slenderness limit for slabs supported on walls is given in Eq. (26):

$$\frac{l_{max}}{d} = \frac{l_{beam}}{d}\sqrt[4]{\frac{1}{1-0.65\,\frac{l_{min}}{l_{max}}}} \tag{26}$$

4. CONCLUSIONS

In this paper, the main changes in the formulations for cracking and deflections introduced in FprEN 1992-1-1:2022 have been presented and justified.

The main changes in the cracking formulation introduce relevant factors to consider several effects that have been ignored or misrepresented in previous formulations. The main effects are the effect of the bond conditions, the uneven distribution of stresses in elements subjected to bending, and the increase in the crack width due to curvature from the level of the bar to the most tensioned fibre. It is shown that their consideration leads to a reduction the scatter of the model when compared to experiments.

For deflection control, the main changes consist in the inclusion of correction for the slenderness limits to deal with slabs supported on columns and supported at the edges and the introduction of a simplified method which allows to obtain a justified value of the deflection from results of a linear elastic calculation. Globally, the changes lead to an improvement of ease-of-use.

Acknowledgements

The authors wish to thank Gintaris Klakauskas and Aleksandr Sokolov for providing the independent test set for the model.

References

[1] CEN, FprEN 1992-1-1:2023 Eurocode 2: Design of concrete structures — Part 1-1: General rules Rules for buildings, bridges and civil engineering structures, Brussels: CEN, 2022. This document is available through the National members of CEN TC250/SC2.

[2] CEN, EN 1992-1-1. Eurocode 2 Design of concrete structures - Part 1-1: General rules and rules for buildings, Brussels: Comité Européen de Normalisation, 2004.

[3] CEN, "EN 1992-3: Eurocode 2 - Design of concrete structures - Part 3: Liquid retaining and containment structures," CEN, Brussels, 2006.

[4] V. Gribniak, D. Bacinskas, R. Kacianauskas, G. Kaklauskas and L. Torres, "Long-term deflections of reinforced concrete elements: accuracy analysis of predictions by different methods," *Mech Time-Depend Mater*, vol. 17, p. 297–313, 2013. https://doi.org/10.1007/s11043-012-9184-y

[5] F. Carneiro Pacheco Marques Guedes and R. Vaz Rodrigues, "The effect of concrete cover on the crack width in reinforced concrete members-a code perspective," in *2nd International Conference on Recent Advances in Nonlinear Models-Design and Rehabilitation of Structures*, Coimbra, 2017.

[6] V. Gribniak, A. Rimkus, A. Pérez Caldentey and A. Sokolov, "Cracking of concrete prisms reinforced with multiple bars in tension–the cover effect," *Engineering Structures*, vol. 220, p. 110979, 2020.

[7] A. Pérez Caldentey, H. Corres Peiretti, J. Peset Irribaren and A. Giraldo Soto, "Cracking of RC members revisited: influence of cover, φ/ρs,ef and stirrup spacing – an experimental and theoretical study," *Structural Concrete*, vol. 16, no. 1, pp. 69-78, 2013. https://doi.org/10.1002/suco.201200016

[8] C. Naotunna, S. Samarakoon and K. Fossa, "Identification of the Influence of Concrete Cover Thickness and ϕ/ρ parameter on crack spacing," in *15th International Conference on Durability of Building Materials and Components*, Online, 2020.

[9] T. Nguyen Viet and D. Schlicke, "Chapter 9.2 - Crack control of prEN1992-1-1: A critical view," in *Meeting of CEN-TC-250/SC2/WG1 March 28-29, 2022*, On-line Meeting, 2022.

[10] L. Steyl, Plastic cracking of concrete and the effect of depth. PhD thesis, Stellenbosch: Stellenbosch University, 2016.

[11] R. Combrinck, L. Steyl and P. Boshoff, "(2018), Interaction between settlement and shrinkage cracking in plastic concrete," *Construction and Building Materials*, vol. 185, pp. 1-11, 2018.

[12] A. Borosnyói and G. Balázs, "Models for flexural cracking in concrete: the state of the art," Structural Concrete, vol. 6, no. 2 , pp. 53-62, 2005. https://doi.org/ 10.1680/STCO.2005.6.2.53

[13] R. García and A. Pérez Caldentey, "Cracking of reinforced concrete: Tension vs. Flexure. Report on cracking tests of large ties.," Technical University of Madrid, Madrid, Spain, 2018.

[14] R. García and A. Pérez Caldentey, "Influence of casting position on cracking behavior of reinforced concrete elements and evaluation of latest proposal for EN-1992 and MC2020: Experimental study," Structural Concrete, 08 April 2022. https://doi.org/10.1002/suco.202100639

[15] A. Pérez Caldentey, A. García, V. Gribniak and A. Rimkus, "Background document to subsection 9.2.4," CEN TC 2650, Madrid, 2020.

[16] fib, Model Code for Concrete Structures 2010, Lausanne: Fédération Internationale du Béton, 2013, p. 434.

[17] H. Hegger, M. Empelmann and S. J. (2015.)., "Weiterentwicklung von Bemessungsund Konstruktionsregeln bei großen Stabdurchmessern (d>32 mm, B500). Verbundfestigkeit und Übergreifungsstöße. Institutsbericht-Nr.: 341/2015.," Instituts für Massivbau der RWTH, Aachen, 2015.

[18] J. Schoening and H. Hegger, "Concrete elements reinforced with large diameters. Bomd behaviour and lapped joints," in *fib Symposium 2015*, Copenhagen, Denmark, 2015.

[19] A. Pérez Caldentey, "Background document to subsection S.5. Surface reinforcement for large bar diameters," CEN, Brussels, 2022.

[20] A. Beldholm Rasmussen, Modelling of reinforced concrete in the serviceability limit state: A study of cracking, stiffness and deflection in flexural members. PhD Thesis, Aarhus: Aarhus University, 2019.

[21] B. B. Broms, "Crack Width and Crack Spacing in Reinforced Concrete Members," *ACI Journal Proceedings*, vol. 62, no. 10, pp. 1237-1256, 1965. http://dx.doi.org/10.14382/epitoanyag-jsbcm.2010.14

[22] A. Clark, "Cracking in Reinforced Concrete Flexural Members.," *ACI Journal, Proc.*, vol. 27, no. 8, p. pp.851–862., 1956.

[23] CUR Dutch Centre for Civil Engineering, "Scheurvoriviing en Doorbiting in gewapend Beton bij Toepassing van geribd Staal. Research and Codes Report no. 37," Ducth Centre for Civil Engineering, 1968.

[24] E. Hognestad, "High Strength Bars as Concrete Reinforcement – Part 2: Control of Flexural," *Journal, PCA Research and Development Laboratories*, vol. 4, pp. 46-63, 1962.

[25] E. Rüsch and G. Rhem, "Versuche mit BetonformStählen. (1963), pt. II (1963), pt. III (1964).," *Deutscher Ausschuss für Stahlbeton*, no. 140, 1963-1964.

[26] J. Farra and J. Jaccoud, "Rapport des Essais de Tirants sous déformation imposée de courte durée.," EPFL, Lausanne, 1996.

[27] A. Rimkus and V. Gribniak, "Experimental Investigation of cracking and deformations of concrete ties reinforced with multiple bars," *Construction and Building Materials*, vol. 148, pp. 49-61, 2017. http://dx.doi.org/10.1016/j.conbuildmat.2017.05.029

[28] A. Pérez Caldentey, R. García, V. Gribniak and A. Rimkus, " Tension versus flexure: Reasons to modify the formulation of MC 2010 for cracking," *Structural Concrete*, vol. 21, p. 2101– 2123, 2020. https://doi.org/10.1002/suco.202000279

[29] V. Gribniak, R. Jakubovskis, A. Rimkus, P.-L. Ng and D. Hui, "Experimental and numerical analysis of strain gradient in tensile concrete prisms reinforced with multiple bars," *Construction and Building Materials*, vol. 187, pp. 572-583, 2018. https://doi.org/10.1016/j.conbuildmat.2018.07.152

[30] R. I. Gilbert and S. Nejadi, "An experimental study of flexural cracking in reinforced concrete members under short term loads. Report.," University of New South Wales, Sidney, Australia, 2015.

[31] E. Calderón Bello, "Estudio experimental de la fisuración en piezas de hormigón armado sometidas a flexión pura. PhD Thesis.," Technical University of Madrid (UPM), Madrid, Spain, 2008.

[32] M. Wu, Tension stiffening in reinforced concrete – instantaneous and time-dependent behaviour. PhD Thesis., Cardiff, Wales: The University of South Wales., 2010.

[33] R. J. Frosch, B. D.T and R. Radabaugh, Investigation of bridge deck cracking in various bridge superstructure systems. Report No. FHWA/IN/JTRP-2002/25., West Lafayette, Indiana: Purdue University, 2003.

[34] C. Base, A. Beeby and P. Taylor, An investigation of the crack control characteristics of various types of bar in reinforced concrete beams. Research report 18., Cement and Concrete Association., 1966.

[35] Klaklauskas, "Personal communication (unpublished)," 2019.

[36] A. Pérez Caldentey, J. Mendoza Cembranos and H. Corres Peiretti, "Slenderness Limits for deflection control: a new formulation for flexural RC elements," *Structural Concrete*, vol. 18, no. 1, pp. 118-127, 2016. https://doi.org/10.1002/suco.201600062